

Analysing MBN signals of different materials by time-frequency methods

Linilson R. Padovese

Department of Mechanical Engineering, School of Engineering,
University of Sao Paulo
Av. Prof. Mello Moraes, 2231
Sao Paulo/SP, 05508-900, Brazil
55 11 3091 5590
55 11 3813 1886
lrpadove@usp.br

Nadine Martin
Julien Huillery

GIPSA-lab, INPG/CNRS
Department Images Signal
Grenoble Campus
BP 46 - 961, rue de la Houille Blanche
F-38402 Saint Martin d'Hères – France
nadine.martin@gipsa-lab.inpg.fr

ABSTRACT

Due to the fact that Magnetic Barkhausen Noise (MBN) carries out information about the microstructure and stress behavior of ferromagnetic steels, it has been using as a basis for effective Non Destructive Testing (NDT) methods, opening new areas in NDT industrial applications. One of the factors that determines the quality and reliability of the MBN analysis is the way information is extracted from the signal. Commonly, simple scalar parameters are used to characterize the information content, such as, amplitude maxima, signal root mean square, and so on. This paper presents a new approach based on the MBN time-frequency analysis. The experimental case that illustrates this approach regards the use of MBN signals to characterize different types of steels. It is shown that, due to non-stationary characteristics of the MBN, time-frequency representations can provide a rich and new panorama of these signals. Extraction techniques of some time-frequency parameters are used to allow a diagnostic process. A comparison with results obtained by the classical method highlights the improvement on the diagnosis provided by the proposed method.

1. INTRODUCTION

The Magnetic Barkhausen Noise (MBN) is a magnetic phenomenon produced when a variable magnetic field induces magnetic domain wall movements in ferromagnetic materials. These movements, not continuous but discrete, are caused by defects in the material microstructure, and generate magnetic pulses that can be measured by a coil placed on the material surface. Since the MBN is sensitive to the state of the material microstructure, to the presence of

deformations and of mechanical stresses, it can be (and has been) used in the development of Non-Destructive Essays regarding several industrial applications [811]. The success in the development of inspection systems based on the MBN depends on the synergetic use of knowledge from different areas such as material sciences, electronics, mechanics, and signal processing.

A point put in evidence by MBN studies is the importance of a deeper study of signal processing methods allowing better highlighting and separation of MBN signal information concerning the various material states.

The traditional MBN signal processing analysis methods can be classified in two classes: the scalar methods (or 0 dimension methods – 0D) and the vector methods (or 1 dimension methods – 1D). The 0D methods use parameters extracted from the MBN signal, such as Root Mean Square (RMS), energy, maximum value, number of MBN peaks at certain values, or else from the frequency domain, such as the energy at some frequency bands. The 1D class uses the envelope of the time signal or that of the spectral MBN signal. As one increases the dimension of the analysis methods, the quality and quantity of the available information carried out by the signal increases.

However, due to the nature of the Barkhausen signal, e.g., a sequence of discrete magnetic pulses whose physical model is sometimes associated to avalanches belonging to the class of critically self-organized phenomena [7], it seems that other methods of signal analysis would be more adequate as, for example, time-scale methods permitting multiple time-frequency scale analysis, instead of linear analysis characterizing the time-frequency methods commonly used in non-stationary phenomena. Very few works have been published about these subjects, related to the Magnetic Nondestructive methods [3,4].

By analyzing the signal envelope and the spectrum, it is observed that the signal is time limited and has a wide spectral band. Several questions remain unanswered by the one dimension analysis. For instance: how is the time-frequency structure of MBN? Is there any time-frequency structure that is related with the evolution of stress or with some microstructure variation in the material? Is there any time-scale structure? Is there some informational gain in relation to the traditional scalar and 1D methods? What are the more adequate method of time-frequency (TFR) and time-scale (TSR) representations, available in the international literature, that better describe the informational content of the MBN signal?

This work presents the traditional methods of MBN signal analysis, and studies the use of some time-frequency and time-scale representations in the analysis of MBN signals measured in four different steels. Section 2 presents the experimental measurements. Section 3 and 4 sum up the time-frequency and time-scale methods we have considered. Section 5 comments the differences between the representations obtained. Section 6 presents the results of the study. In Section 7, a first result of automatic detection in the time-frequency plan is presented.

2. EXPERIMENTAL MEASUREMENTS

Samples of four different steels were used in the experiments: a high carbon AISI 1070, a pipeline steel X80, a tool steel AISI D2 and a ARBL steel (High Strength Low Alloy steel). In each sample, 6 MBN responses were measured.

Figure 1 shows a flow chart of the measurement arrangement. A Personal Computer with a data acquisition device (with A/D, D/A and D/D channels) supplies a sinusoidal wave of 10 Hz, which is amplified by a bipolar source, This source feeds the magnetic circuit in order to magnetize the sample with a magnetic field, inducing saturation in the samples. The MBN sensor output is amplified, band pass filtered (1 - 100 kHz) and digitalized with a sampling frequency of 200 kHz. Each signal records the magnetic response of 2 cycles of the magnetic excitation.

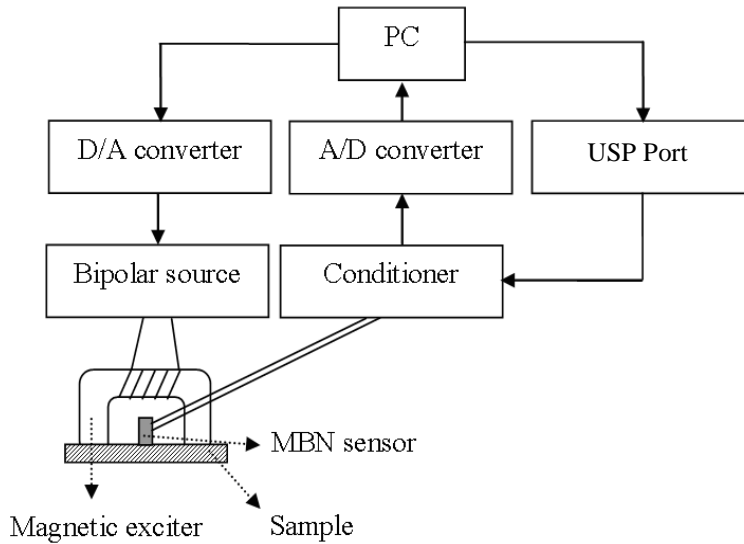


Figure. 1 Experimental setup for MBN signal measurements.

3. TIME-FREQUENCY REPRESENTATIONS

Time-frequency representations are characterized by a fixed resolution in all the time-frequency plan. We have considered 4 of them:

- the spectrogram, the more classical and the more robust;
- the Wigner-Ville and its smoothed version, which belong to the same class than the periodogram, the Cohen class, and well known for its higher resolution and the presence of interference;
- the Capongram, middle between the Cohen class and the parametric representation, interesting for good statistical properties at the expense of computing time;
- the ARgram, a parametric approach.

The latter two have been adapted to nonstationary signals by a simple gliding time window.

3.1 Spectrogram

A linear TFR based on the Fourier transform can be reached by pre-windowing the signal around a chosen time, calculating its Fourier Transform, and proceeding in the same way for each instant. This transform is known as Short Time-Frequency Transform and referred to as STFT(t,f) where t is the time variable and f the frequency variable. A quadratic form related with the Short Time-Frequency Transform can be obtained by taking the square of this transform. It is known as spectrogram and measures the spectral energy density of the signal in the time-frequency plan. The spectrogram of a signal x(t) is referred to as SPECT(t,f). The following holds

$$\text{SPEC}(t,f) = \left| \text{STFT}(t,f) \right|^2 = \left| \int_{-\infty}^{\infty} x(\tau) h^*(\tau-t) e^{-j 2 \pi f \tau} d\tau \right|^2, \quad (1)$$

where h(t) is a sliding weighting window and the superscript * denotes conjugate.

The time resolution of the spectrogram is determined by the length of the selected sliding window h(t), and the frequency resolution is defined as the -3 dB bandwidth of the spectral window, the spectral window being the spectrogram of the window h(t). The best frequency resolution is achieved with the natural window and defined as $\Delta f = 1/D$, where D is the time duration of the window. Any other different window will degrade the resolution but improve the

estimation variance. The product $\Delta f \times D \geq 1$ measures the joint time-frequency resolution of the method. This resolution limitation is the most significant drawback of the spectrogram. Other major problems can be cited: (a) the implicit windowing problem that causes the “leakage” phenomenon, and (b) the impossibility of averaging periodograms for reducing the estimation variance when working with short data. Nevertheless one advantage of this method is its robustness towards the nature of the signal.

3.2 WV and SPWV

The Cohen class is a general formulation for non-parametric time-frequency distribution, which includes the Wigner-Ville Distribution and relatives. The spectrogram can be considered as a special case of the Cohen class. The Wigner-Ville Distribution of a signal $x(t)$ is referred to as WVD(t,f) and can be defined as [6]

$$\text{WVD}(t,f) = \int_{-\infty}^{\infty} x(t + \tau/2) x^*(t - \tau/2) e^{-j 2\pi f \tau} d\tau. \quad (2)$$

Since the value of the WVD(t,f) is determined by all the values of the signal (and therefore, not limited by a time window), the Wigner-Ville Distribution overcomes the spectrogram tradeoff between time and frequency resolution, the hypothesis of short-term stationarity is no more necessary. This improvement comes at a price of the appearance of spectral cross-terms, which comes from the bilinear kernel of the transform. This spectral interference is critical in multicomponent signals, since it makes difficult the distinction of weaker signal components and it masks spectral features.

To overcome this major drawback, several modifications have been proposed and can be found in the literature. One of them, the Smooth Pseudo Wigner Ville Distribution is of particular interest to this work since it will be used later to analyse experimental results. The Smooth Pseudo Wigner Ville Distribution of a signal $x(t)$ referred to as SPWV(t,f) can be defined as [6]

$$\text{SPWVD}(t,f) = \int_{-\infty}^{\infty} h(\tau) \int_{-\infty}^{\infty} g(t - \eta) x(\eta + \tau/2) x^*(\eta - \tau/2) d\eta e^{-j 2\pi f \tau} d\tau, \quad (3)$$

where $g(t)$ is the time smoothing window and $h(t)$ the frequency smoothing window. With the introduction of these two windows it is possible to attenuate and to smooth the interference terms of the Wigner-Ville distribution, by independently choosing the type of window and its length.

3.3 Capongram

The Capon Method or Minimum Variance Method is a nonparametric spectral power estimator having higher frequency resolution than the Fourier Transform based methods. The quantity estimated, homogeneous to the power of signal $x(t)$, is referred to as $P_{CAP}(t,f)$ and is defined by [12]

$$P_{CAP}(t, f) = \frac{1}{\mathbf{e}_p^H(f) \mathbf{R}_p^{-1}(t) \mathbf{e}_p(f)}, \quad (4)$$

where $\mathbf{e}_p^T = (1, e^{-2\pi i f ts}, \dots, e^{-2\pi i f p ts})$, ts is the sample interval, the superscripts H denotes conjugate transpose, p is the order of the Capon filter. $\mathbf{R}_p(t)$ is the correlation matrix of dimension $(p+1) \times (p+1)$ evaluated on a gliding time window centred at the time instant t .

The signal power obtained by this approach can be seen as the output of a filter, of length p and with variable center frequency. Parameter p has to be chosen by the user.

The design of the Capon method allows the frequency resolution to be high on a short time window. This approach assumes signal stationarity over the time window and, therefore, is appropriated to analyze weakly non-stationary signals.

3.4 ARgram

The gliding power spectrum density of the Autoregressive Model of a signal $x(n)$, referred to as $S_{AR}(t,f)$, can be obtained by [13]

$$S_{AR}(t,f) = \frac{P_w}{\left| 1 + \sum_{k=1}^p a_{k,t} e^{-j2\pi f k} \right|^2}, \quad (5)$$

where P_w is the power of the white noise (or the prediction error), p is the model order and $a_{k,t}$, the model coefficients evaluated on a time gliding window centred at t . This equation is also known as the Maximum Entropy Spectrum. The choice of the order p is done by the user and constitutes the main issue of this approach.

As for the Capon method, the AR model allows the frequency resolution to be high on a short time window. This approach assumes signal stationarity over the time window and, therefore, is appropriated to analyze weakly non-stationary signals

4. TIME-SCALE REPRESENTATION

Two time-scale transform have been considered:

- a scalogram as a classical time-scale transform;
- a Mellogram as an adaptation of the Mellin transform for nonstationary signals.

4.2 Scalogram

The Scalogram is a time-scale representation based on the Wavelet Transform, referred to as $Tx(t,a;\Psi)$ and defined by [6]

$$Tx(t,a;\Psi) = \int_{-\infty}^{\infty} x(s)\Psi_{t,a}(s)ds, \quad (6)$$

where $\Psi_{t,a}(s) = |a|^{-1/2} \Psi\left(\frac{s-t}{a}\right)$, and Ψ is the mother wavelet. Parameter a is the scale factor.

Although the representation obtained is time-scale, it is possible to establish an associated time-frequency representation, by using the relation $f = f_0/a$, where f_0 is a reference frequency of the mother wavelet.

4.2 Mellogram

Several transforms have been proposed in order to operate a dominium transformation, with the objective of facilitating interpretation of a physical phenomenon. One of these transforms is the Mellin Transform. The gliding Mellin transform of a signal $x(t)$ referred to a $M_x(t;p)$, can be deduced from its general form [1,2] and is given by

$$M_x(t;p) = \int_0^{\infty} x(\tau)w(t-\tau)t^{p-1}d\tau, \quad (7)$$

where p , a complex number, is the Mellin parameter and $w(t)$ a time window.

A particular form of the Mellin transform, also named Scale Transform, is obtained by using $p = -jc+1/2$, with c a real number. Therefore, adapted to nonstationary signals, a gliding Scale transform, referred to as $D_x(t;c)$, is

$$D_x(t;c) = \frac{1}{\sqrt{2\pi}} \int_0^{\infty} x(\tau)w(t-\tau)e^{(-jc-1/2)\ln\tau}d\tau. \quad (8)$$

If $x(t)$ is a function and $g(t)$ is a scaled version of $x(t)$, then the amplitude of the transform will be the same. If $x(t)$ has a scale periodicity of period τ , then $x(t) = \sqrt{\tau}x(\tau t)$.

5. VANTAGES AND DISADVANTAGES OF EACH METHOD

Table 1 presents the values of the parameters used in each method to calculate the TFRs, and the computational time consumption for each case.

The Spectrogram in (1) is fast and very easy to use, since the transform does not depend on some *a priori* information (order parameter) as in ARgram and Capongram cases. But the estimation has the highest variance and the lowest time-frequency resolution.

The Wigner-Ville distribution (2) presents two major advantages: it is a non-parametric method and it has a good time-frequency resolution.. Its major drawback is the appearance of spectral cross-terms, which makes difficult the distinction of weaker signal components. Additionally, it masks spectral features.

The Smoothed Pseudo Wigner-Ville distribution defined in (3) attenuates and smoothes the interference terms, at a cost of some degradation in time-frequency resolution. However, these two methods have a severe limitation related with the computational memory consumption. The amount of memory used in all the analyses was the same, but was not enough for the Wigner-Ville distribution and Smoothed Pseudo Wigner-Ville distribution given the length of the recorded signals (see Table 1).

Therefore the authors have considered these two methods are not competitive in face of the other ones, and they were abandoned.

Table 1. Parameters used in the TFR and TSR calculations (microprocessor Centrino 1.8 GHz, 1 GB RAM).

TFR	Parameters	Computational Time
Spectrogram	$N_{win}=512; N_{overlap}=128;$	0.35
Capongram	$N_{win}=512; N_{overlap}=128; order=100$	108
ARgram	$N_{win}=512; N_{overlap}=128;$ $Order=40$	10.3
Scalogram	$Number\ of\ scales=50$	165
Mellinogram	$N_{win}=512; N_{overlap}=128;$	9.1

Capongram (4) has a higher time-frequency resolution and lower variance than Spectrogram, but is more computationally time consuming than this last one and the ARgram method (see Table 1). Although the Capongram does not impose a model in the signal, it is necessary to estimate a parameter, named “order” p that has a meaning different from the order of the ARgram. Meanwhile the AR model order is related with the degree of freedom of the system being modelled, the Capongram order describes the filter length. In the AR model, the order is optimal when its value is close to the system degree of freedom, whereas an increase in the Capon filter bank order increases the frequency resolution at the expense of deterioration of statistical stability.

In other words, in the ARgram method the spectral information is contained inside the AR filter and, conversely, is in the output of the filter in the Capongram method

The ARgram (5) is a time–frequency method more adequate to describe narrow band spectral components. The main drawback of this method is, maybe, that it implies an *a priori* knowledge

(or assumption) about the process from which the signal is taken. This *a priori* information is expressed by the selection of the model order p . A good choice of this parameter is essential for good spectral estimation, what implies an additional computational time in order to find a good value (see Table 1). Other disadvantage is the high computing time necessary to calculate the spectrum in each time moving window (see Table 1). The main advantage of the ARgram method is its high time and frequency resolution and its low variance.

Although very time consuming, the highest among the used methods, the Scalogram (6) is simple to use, depending only on the choice of the number of analysis scales. Both, the Scalogram and Mellingram (8), are methods that can show scale structures in the signal, if they exist and in a different manner, not identifiable with the traditional time-frequency representations.

6. RESULTS

In what follows some results of experimental database analysis are shown in a sequence of increasing richness of information representation and, by consequence, also of increasing complexity of analysis and interpretation.

Figure 2 shows the 4 MBN signals, for each type of steel, plotted in the same scale, for amplitude comparison. It is possible to notice that, for the same magnetic excitation, each material responds in a different manner. The aim of the signal processing process is to put in evidence the details of the MBN behaviour differences among them.

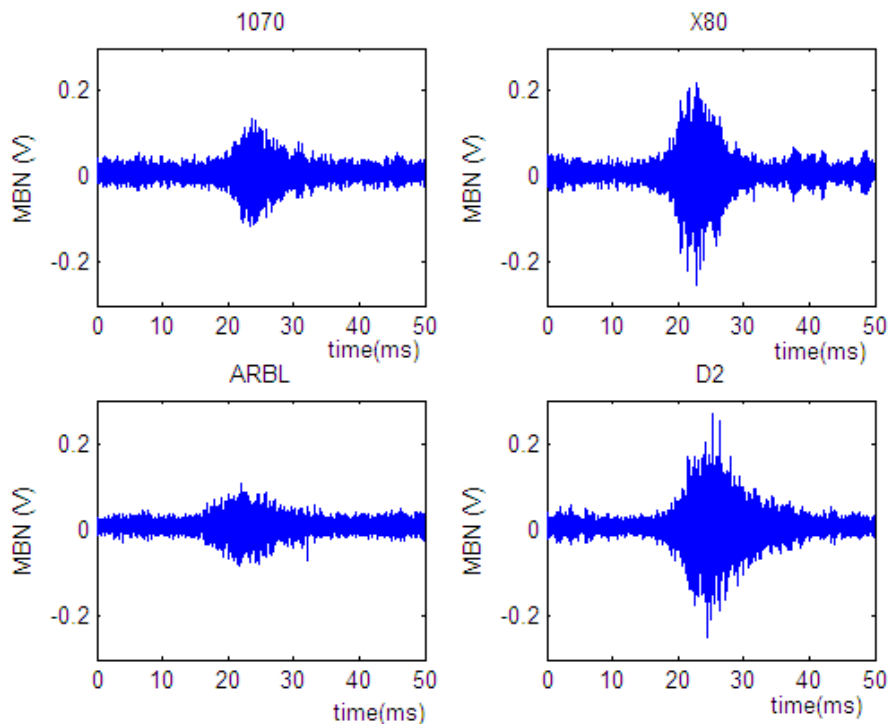


Figure 2. MBN signals for different materials

Figure 3 shows the average of 6 MBN RMS values, for each type of steel. It's worth noting that X80 and D2 are hardly distinguished by this approach.

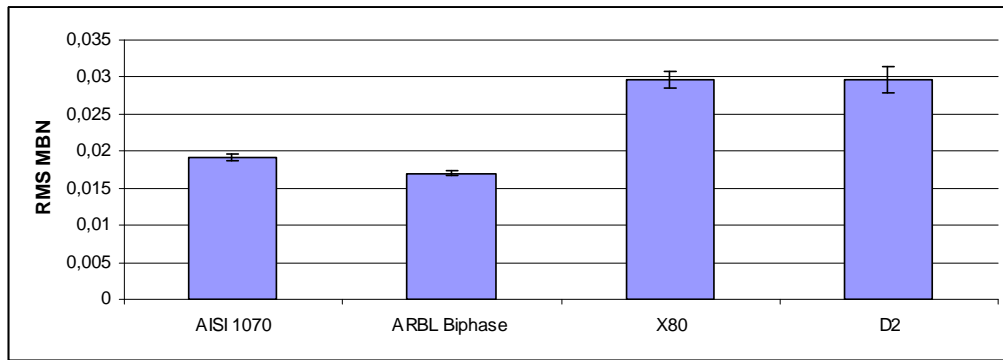


Figure 3. RMS MBN for different materials

Figure 4 presents the average envelope of the MBN signal and the average envelope of the MBN spectrum. Since this kind of representation gives more information than the scalar parameters, the difference among the steels is more apparent.

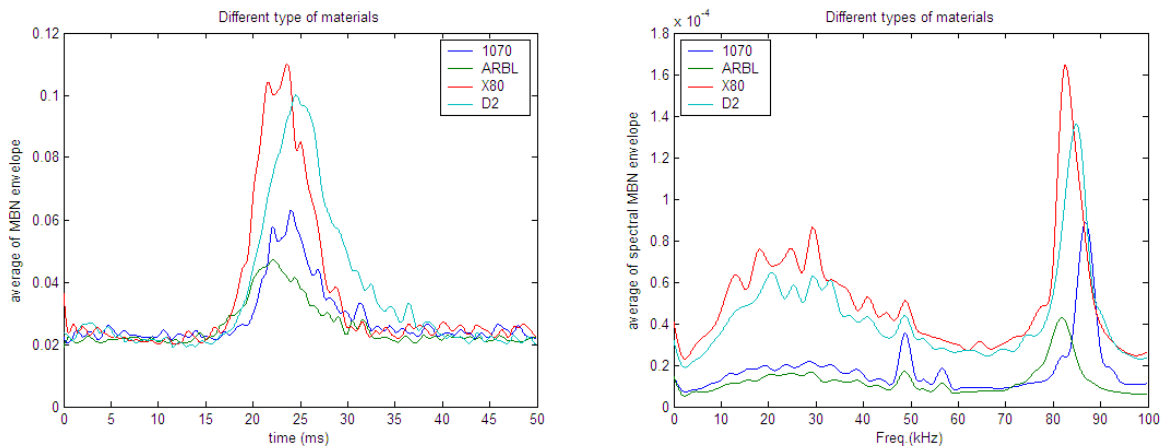


Figure 4. a) Average envelope of MBN signals; b) Average envelope of MBN spectra

However, we will show that the TFRs and TSRs are much richer in details than the scalar parameters and envelope representations. The TFRs and TSRs were calculated for all the four steels types, but, due to space limitation in this paper, only the results for the D2 steel are shown.

It is important to know that significant improvement in the quality of the TFRs representations can be reached by using averages of TFRs or TSRs. Therefore, all TFRs images shown in Figure 5 and 6 are averaged over 6 TFRs evaluated on successive measurements of the same phenomenon and are presented with the same z-axis scale, in order to allow comparison among them.

By analysing the graphical representations of Figure 5, it is interesting to notice that the Scalogram results are very similar to the TFRs ones. This means that there is no scale phenomenon, at least perceptible in this representation, in the MBN signals. Additionally, by analysing the Mellingram results, no scale structure could also be detected. Therefore, it seems that TFRs are enough to describe the informational content of MBN signals.

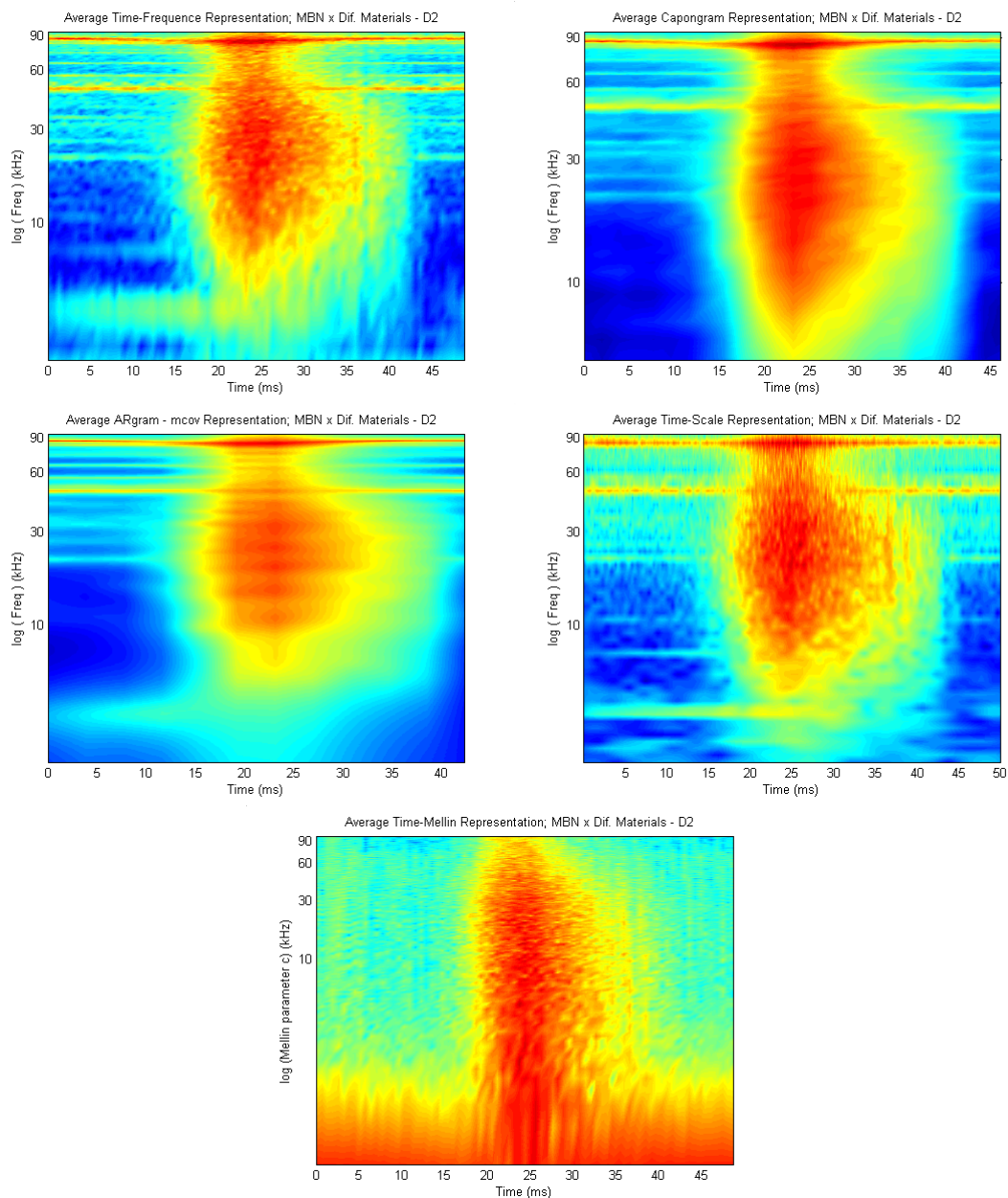


Figure 5. TFRs of D2 steel: a) Spectrogram; b) Capongram; c) ARgram; d) Scalogram; e) Mellinogram

In Figure 6, the TFR of each one of the four steels is shown.

Two main kinds of information can be taken from Figure 6. First several almost stationary narrow-band components, close to 50 kHz and 90 kHz, are visible all over the time duration of the signal). These frequencies cannot be related to MBN phenomenon and may come from some external interferences of the measurement equipment. Although these frequencies can be observed in the envelope of the MBN spectrum (Figure 4), their stationary nature, noticed only in the TFRs, allow concluding that they are not related to the MBN phenomenon.

Second, the remaining information is on the non-stationarity part of the MBN signals. All the information presented in the MBN envelope and in the envelope of the MBN spectrum is combined in a synergetic way, resulting in the richest panorama that can be seen in the TFR's of Figure 6.

The differences among the MBN behaviours, for each steel, are clearly noticeable, mainly the shape of the spectral pattern, amplitudes, time and frequency distribution.

As a result, the authors choose the Capongram among the TFR's and TSR's taken in consideration in this paper, since this representation is able to highlight the differences between the four different steels studied.

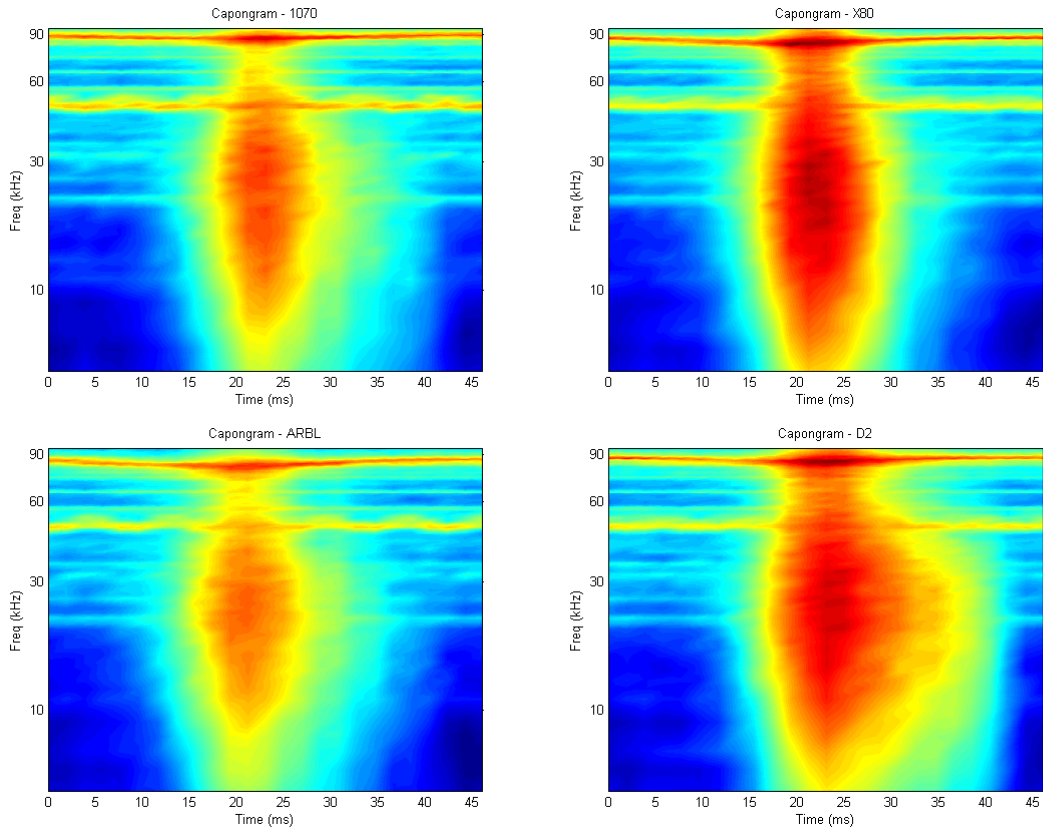


Figure 6. Average of Capongram TFR for steels (in clockwise direction): a) 1070; b) X80; c) ARBL; d) D2

7. A TIME-FREQUENCY SOURCE SEPARATION

This section is a first result in order to introduce future works, which will naturally attempt to propose an automatic diagnosis using time-frequency representations. As noted in section 0, a time-frequency representation of the MBN records shows two types of time-frequency patterns. In addition of the MBN, some components are visible and may come from some external interferences of the measurement equipment. The purpose of this section is to apply a method proposed in [14-15], which allows an automatic detection of the time-frequency patterns according to the assumption of what we decide to be the noise. In this MBN application, the signal of interest is in fact the noise, the MBN, whereas the electronic perturbations are the noise. We will then launch the method under the assumption of a non-stationary and non-white noise in order to detect the MBN signal in the noise part of the signal.

The derivation of the method is out of the scope of this paper. Further details should be found in [14-15]. According to the progress of the development, we are not still able to present results on the Capongram but only on the spectrogram. Then, Figure 7 shows the results of the time-frequency detection when applied on the spectrogram of the D2 steel on a longer duration than in Figure 5. The time-frequency plan in the upper right side is then an estimation of the MBN signal only. As a complement, the time-frequency plan in the lower right side gives the result of the detection of the components mixed with the MBN that is the electronic interferences. For getting the algorithm need no more *a priori* information than the properties of non-stationarity and non-whiteness of the noise.

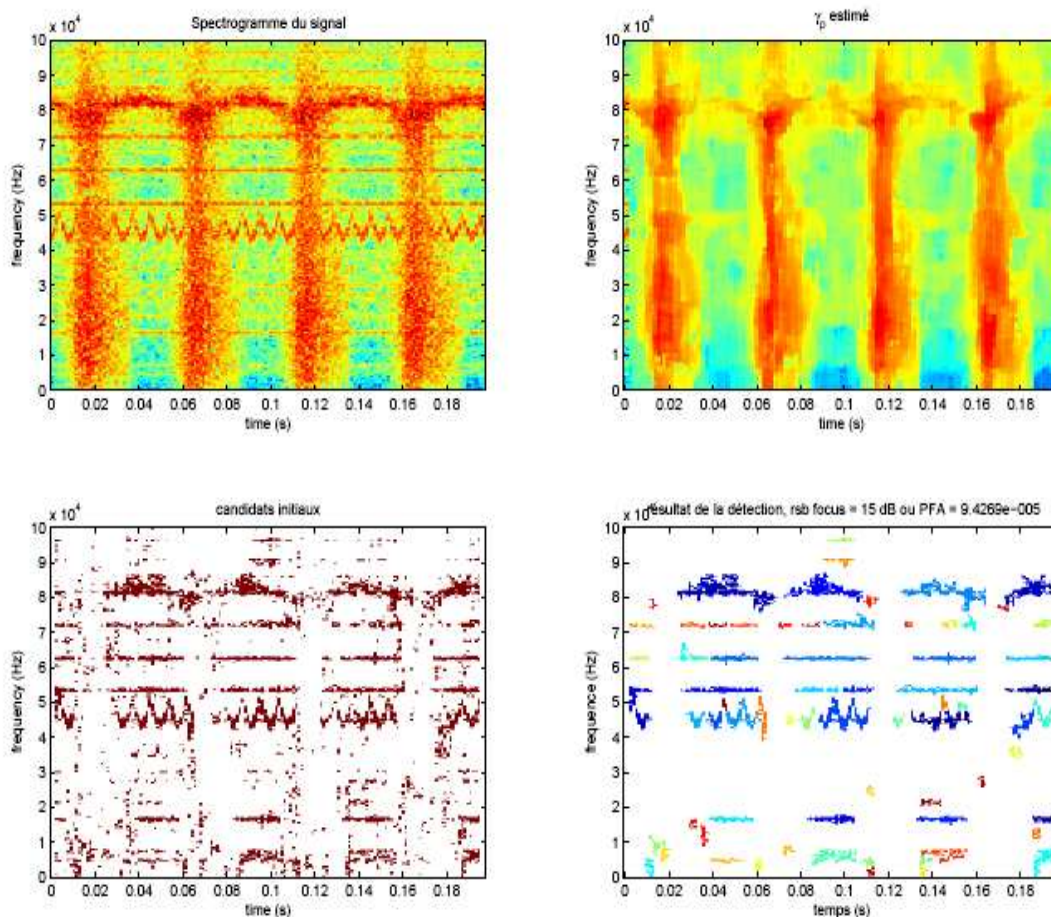


Figure 7. Source separation by detection in the Spectrogram of D2 steel: spectrogram (top left), noise estimation –top right), candidates for detection (bottom left) and detection result (bottom right)

8. CONCLUSIONS

Three Time-Frequency Representations and two Time-Scale Representations were used in order to analyse Magnetic Barkhausen Noise signals measured in four different steels. The vantages and disadvantages of each method are commented. TFRs and TSRs images of same steel and images of a TFR method for four different steels are presented. These results allow higher information quality for the MBN phenomenon than the traditional methods. Additionally, the TSRs did not show scales structures in the MBN signals.

Although the TFR method can supply rich information on the MBN signals very few studies were undertaken with TFRs methods in this magnetic phenomenon. On other hand, the richer the quality of the information, the harder the analysis and the comparison of different cases, for the amount of information is high.

Therefore, future works should emphasize the development of methods of extraction of image characteristics, in order to allow classification tasks by means of MBN TFRs information.

Acknowledgements

The authors want to thank FAPESP (05/51100-9 and 06/04935-0) for the financial support and Eng. Freddy Franco for his add in the MBN measurements.

References

1. De Sena A.; *La Trasformata di Mellin: teoria ed applicazioni all'analisi di segnali audio*; Tesi de Laurea, Università degli Studi de Verona, 2003.
2. De Sena, A.; Rocchesso D.; *A Fast Mellin and Scale Transform*; EURASIP Journal on Advances in Signal Processing; Vol. 2007, Article ID 89170, 9 pages.
3. Magalas, L. B.; *Application of the wavelet transform in mechanical spectroscopy and in Barkhausen noise analysis*; Journal of Alloys and Compounds 310 (2000) 269–275.
4. Peter Maass, Gerd Teschke, Werner Willmann, and Günter Wollmann; *Detection and classification of Material Attributes—A Practical Application of Wavelet Analysis*; IEEE Trans. On Signal Processing, 48, August 2000.
5. Padovese, L.R.; *Hybrid time-frequency methods for non-stationary mechanical signal analysis*; Mechanical Systems and Signal Processing, v.18, p.1047 - 1064, 2004.
6. P. Flandrin,; *Time-frequency/time scale*, Academic Press, S. Diego, 1999.
7. Urbach, JS; Madison, RD; Markert, J; *Interface Depinning, Self-Organized Criticality, and the Barkhausen effect*; Physical Review Letters; 75(2), p. 276-279, 1995.
8. Pérez-Benitez, J. ; Capo-Sanchez, J. ; Anglada J. R. ; Padovese, L. R. *A study of plastic deformation around a defect using the Magnetic Barkhausen Noise in ASTM 36 steel*. NDT & E International, v. 41, p. 53-58, 2008.
9. Capo-Sanchez, J; Alberteris-Campos, M.; Padovese, L.R.; *Magnetic Barkhausen measurements for evaluating the formation of Lüders bands in carbon steel*, NDT & E Intern., 40, p. 520-524, 2007.
10. Altpeter I. *Nondestructive evaluation of cementite content in steel and white cast iron using inductive Barkhausen noise*. Journal of Nondestructive Evaluation. 1996; 15 (2); 45-60.
11. Lachmann C, Nitschke-Pagel Th, Wohlfahrt, H. *Characterisation of residual stress Relaxation in Fatigue Loaded Welded Joints by X-Ray Diffraction and Barkhausen Noise Method*. Materials Science Forum. 2000;V 347-349, 374-379.
12. N. Martin, *Minimum Variance*, Chapter 7, pp. 175-211. Book « Spectral Analysis », Edited by F. Castanié. Traité IC2, Editeur HERMES, pp 175-211, May 2006.
13. N. Martin, *An AR Spectral Analysis of Non Stationary Signals*. Signal Processing, 10, pp. 61-74, January 1986.
14. J. Huillery, *Time-frequency support of an unknown signal embedded in an additive Gaussian noise*, PhD Thesis, INPG, Grenoble, 9 July 2008 (in French).
15. J. Huillery, Martin N., *A Bayesian Approach for the Detection of Time-Frequency Components of Signals*, Seventh International Conference on Mathematics in Signal Processing, IMA 2006, Royal Agricultural College, Cirencester, UK., 17-20 December 2006